View metadata, citation and similar papers at core.ac.uk
brought to you by CORE
provided by Elsevier - Publisher Connector

Poster Viewing: 7: Physics: Intra-fraction motion management II

PV-0322

Target displacement evaluation for fluoroscopic and four-dimensional cone-beam computed tomography

H. Iramina[1], M. Nakamura[2], Y. Iizuka[2], Y. Matsuo[2], T. Mizowaki[2], M. Hiraoka[2], I. Kanno[1]
[1]*Kyoto University, Nuclear Engineering, Kyoto, Japan*
[2]*Kyoto University, Radiation Oncology and Image-Applied Therapy, Kyoto, Japan*

Purpose or Objective: Four-dimensional cone-beam computed tomography (4D-CBCT) has great capability to provide volumetric and respiratory motion information with one gantry rotation. It is necessary to quantitatively assess, how difference of tumor displacement between actual and 4D-CBCT image exists. In this study, we evaluated the displacement of implanted fiducial markers assumed as tumor on fluoroscopic projection images and reconstructed 4D-CBCT images with different sorting methods.

Material and Methods: We have developed 4D-CBCT utilizing dual source kV X-ray imaging subsystems. Five lung cancer patients with two to four implanted fiducial markers were enrolled in the institutional review board-approved trial. Each patient underwent three consecutive 4D-CBCT imaging. For at least two scans out of three, the imaging parameters were 110 kV, 160 mA and 5 ms, the rotational speed of the gantry was 1.5°/s, rotation time was 70 s, the image acquisition interval was 0.3°, and the rotational angle of 105°. A marker that located the most nearest to the lung tumor was used for surrogate respiratory signal. The marker motion in superior-inferior (SI) direction was used as surrogate respiratory signal for 4D-CBCT image reconstruction. Surrogate respiratory signal were converted eight phase bins with retrospective amplitude- or phase-based sorting. On reconstructed 4D-CBCT images, the marker was contoured on all phases to detect its 3D positions. Meanwhile, the marker positions on two fluoroscopic images obtained simultaneously were converted to 3D position. Evaluation was employed among the displacement on fluoroscopic image (*d*fluoro), that on amplitude-based sorting 4D-CBCT (*d*a-4DCBCT) and that on phase-based sorting 4D-CBCT (*d*p-4DCBCT) in left-right (LR), anterior-posterior (AP), and SI direction. Difference between *d*a-4DCBCT and *d*fluoro (*D*a-f), and difference between *d*p-4DCBCT and *d*fluoro (*D*p-f) were obtained for all patients.

Results: Depending on the sorting methods, the positional difference was up to 2 mm on 4D-CBCT images. Overall mean ± standard deviation of *D*a-f and *D*p-f in LR, AP, and SI direction were -1.5±1.2, -2.9±1.2, -5.1±1.6 mm and -1.4±1.1, -2.3±0.9, -5.2±1.2 mm, respectively (Table 1). 4D-CBCT underestimated displacement of marker by 5 mm on average in SI direction.

Table 1. Means and standard deviations of $D_{a\text{-}f}$ and $D_{p\text{-}f}$ for LR, AP, and SI direction.

Sorting	Patient	1st			2nd			3rd		
		LR	AP	SI	LR	AP	SI	LR	AP	SI
Amplitude -based	1	-1.0	-3.2	-4.3	-0.5	-5.8	-4.0	-1.5	-3.0	-5.3
	2	-0.2	-3.3	-7.8	-0.7	-1.3	-4.3	-1.3	-2.9	-5.4
	3	-4.2	-1.7	-3.9	N/A	N/A	N/A	-2.8	-2.6	-4.3
	4	-0.4	-1.3	-2.6	N/A	N/A	N/A	-0.9	-2.5	-4.1
	5	-2.0	-2.7	-7.4	N/A	N/A	N/A	-2.9	-3.8	-7.4
	Mean	-1.6	-2.4	-5.2	-0.6	-3.6	-4.1	-1.9	-3.0	-5.3
	SD	1.5	0.8	2.1	0.1	2.3	0.1	0.8	0.5	1.2
Phase -based	1	-1.2	-2.0	-4.3	-0.6	-4.4	-5.4	-0.8	-1.7	-4.8
	2	0.5	-1.8	-5.8	-0.1	-2.0	-5.3	-1.5	-2.0	-5.3
	3	-3.6	-1.3	-4.9	N/A	N/A	N/A	-1.9	-2.1	-4.8
	4	-0.6	-1.6	-3.1	N/A	N/A	N/A	-1.1	-2.6	-4.1
	5	-2.3	-2.8	-6.4	N/A	N/A	N/A	-3.0	-3.8	-8.0
	Mean	-1.5	-1.9	-4.9	-0.4	-3.2	-5.4	-1.7	-2.4	-5.4
	SD	1.4	0.5	1.2	0.2	1.2	0.1	0.8	0.7	1.4

Abbreviations; LR: left-right, AP: anterior-posterior, SI: superior-inferior, SD: standard deviation, N/A: not available
Note: For Patient 3 to 5, 4D-CBCT images at 2nd session was taken for different purpose with different imaging conditions from others.

Conclusion: We performed displacement evaluation of fiducial markers on 4D-CBCT with two sorting methods. Since 4D-CBCT requires convolution of marker motion in eight bins, underestimation of 5 mm on average was observed in SI direction.

PV-0323

Prospective evaluation of markerless tumour tracking using 4D3D registration and dual energy imaging

J. Dhont[1], D. Verellen[1], K. Poels[2], M. Burghelea[1], K. Tournel[1], T. Gevaert[1], B. Engels[1], C. Collen[1], R. Van Den Begin[1], G. Storme[1], M. De Ridder[1]
[1]*Universitair Ziekenhuis Brussel, Radiotherapy, Brussels, Belgium*
[2]*Universitair Ziekenhuis Leuven, Radiotherapy, Leuven, Belgium*

Purpose or Objective: Image registration of Digitally Reconstructed Radiographs (DRRs) and real-time kV images is the only clinically implemented solution to markerless tumor tracking. However, registration still suffers from poor soft tissue visibility, restricting the workflow to only a certain size and density of tumors. The purpose of this study is to evaluate the feasibility of markerless tumor tracking on a clinical system through 4D/3D registration and the use of dual-energy (DE) imaging.

Material and Methods: For 3 patients treated for NSCLC with dynamic tracking on the Vero SBRT system, on average 90 soft-tissue enhanced DE images were created from sequential low- (LE) and high-energy (HE) orthogonal fluoroscopy. All DE images were binned in either inhale, exhale, maximum inhale or maximum exhale, using the amplitude of the synchronous external breathing signal.
For each respective breathing phase, DRR templates were created from the 4D planning CT using the open-source Insight Toolkit (itk).
As such, the localization problem was reduced to 2D/2D registration of 2 orthogonal kV images and 2 DRRs.
Before registration, the currently implanted marker was removed on all images so to not bias the results.
Intensity-based 2D/2D registration was carried out between each DE image and the respective DRR. The same was done with all HE images to evaluate the benefit of using DE imaging..
The implanted marker was recovered and used as a benchmark to quantify the accuracy of the tumor localization. The mean Euclidean distance between the center of the marker in the DE and HE images, and the center of the marker in the matched DRR template was defined as the tracking error (TE).

Results: Table 1 summarizes the localization results for each patient and imaging angle. All TEs remain below 2.5 mm and results between DRR-HE and DRR-DE are similar. However, a significant difference in TE is present for 1 imaging angle. From a qualitative analysis, see Figure 1, it can be observed that for those imaging angles where the tumor is mainly obscured by bony anatomy, tumor localization through intensity based registration is more accurate when dual-energy images are applied.

Figure 1 High-energy (left) and dual-energy (right) images from patient 1. Note that the tumour, indicated by the implanted marker, is obscured by soft tissue only for imager 1 (above), while for imaging angle 2 the tumour is mostly obscured by the ribs.

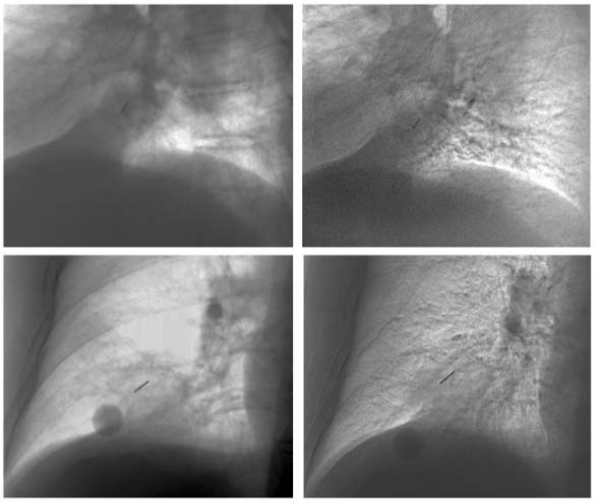

Table 1 Root-mean square (RMS) tracking errors, defined based on the implanted marker distance, from 2D/2D registration between DRR and dual-energy images, and DRR and high-energy images.

	RMS tracking error		
	DRR - DE	DRR - HE	t-test
patient 1 Im. 1 - 10°	1.7 ± 0.8	2.2 ± 0.8	p = 0.08
patient 1 Im. 2 - 100°	1.2 ± 0.6	1.3 ± 0.5	p = 0.83
patient 2 Im. 1 - 70°	1.8 ± 0.7	3.1 ± 1.1	p < 0.01
patient 2 Im. 2 – 340 °	1.4 ± 0.5	1.6 ± 0.8	p = 0.78
patient 3 Im. 1 - 250°	1.3 ± 0.4	1.2 ± 0.4	p = 0.85
patient 3 Im. 2 - 160°	1.3 ± 0.4	2.1 ± 0.5	p = 0.06

Conclusion: The results of this prospective evaluation indicate that for markerless localization of lung tumors through 4D/3D intensity-based registration, using DE images is more accurate than using regular kV images for certain imaging angles. Removing overlying bony anatomy and enhancing tumor visualization prior to registration makes the workflow more robust.

PV-0324

Intra-fraction motion characterisation of head-and-neck tumors using cine-MRI

T. Bruijnen[1], B. Stemkens[1], M.E.P. Philippens[1], L.P.W. Canjels[1], R.H.N. Tijssen[1], T. Schakel[1], C.H.J. Terhaard[1], J.J.W. Lagendijk[1], C.P.J. Raaijmakers[1]
[1]University Medical Center Utrecht, Radiotherapy, Utrecht, The Netherlands

Purpose or Objective: Intensity modulated radiotherapy and the recent introduction of the MR-linac emphasize the need for detailed tumor motion characterization for adequate motion management in radiotherapy planning and online MRI-guidance. Hitherto, intra-fraction head-and-neck (H&N) tumor motion has been assessed as the displacement of local landmarks in cone beam CT or X-ray. The superior soft-tissue contrast of MRI enables characterization of the actual tumor displacement. Here, we investigate the intra-fraction tumor displacement on a sub-second and 10-minute time scale, using cine-MRI.

Material and Methods: Thirteen patients with H&N squamous cell carcinoma underwent pretreatment clinical MR imaging in a radiotherapy immobilization mask. Two 2D sagittal cine-MR scans (balanced steady state free precession; TE/TR = 1.2/2.5 ms; 1.42x1.42mm², slice thickness 10 mm, 500 dynamics), positioned through the tumor were acquired with 8 frames per second and an interval of 10-15 min on a 3.0T MR scanner. Tumor GTVs were delineated by a radiation oncologist.
Image analysis: Tumor motion was estimated by non-rigid image registration over the 1 minute dynamic MRI data using an optical flow algorithm (Fig. 1a). The displacement vectors on the GTV border were combined into a 95th percentile distance (dist95%) for every image. 95% of the range of dist95% over time was used as a measure of tumor displacement. The standard deviation of the GTV border displacement vectors was calculated and averaged over the time series as a measure of tumor deformation. Tumor displacement over 10 minutes was estimated by computing the difference in the average tumor position between the two dynamic series with an equivalent non-rigid registration.

Results: Results of the image registration (Fig. 1c) showed respiratory-induced tumor motion, which was confirmed by a peak at the principle respiratory frequency in a power spectrum analysis. Displacements were relatively small in both directions with a median displacement of 0.60 ± 0.13 mm (range: 0.18–1.44 mm) (AP) and 0.59 ± 0.11 mm (range: 0.32-2.69 mm) (CC) (Fig. 1b), which agreed with visual inspection. For two patients standard deviations within the border pixels were > 0.20 mm, which might imply a deformation of the tumor. The average tumor position differences over 10 minutes were smaller than the tumor displacement in the 1-minute data for both directions, with means of 0.28 mm (range: 0.08-0.99 mm) (AP) and 0.34 mm (range: 0.07-0.99 mm) (CC).

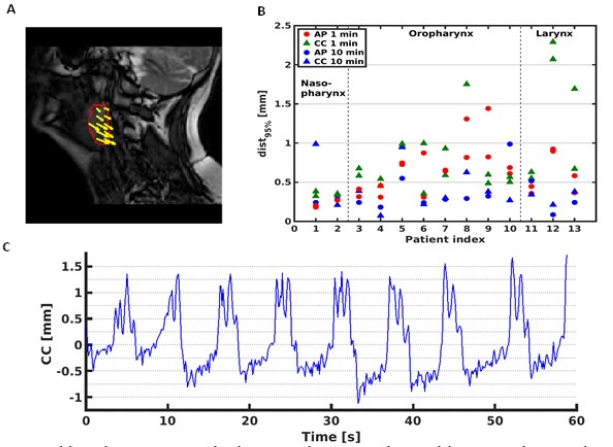

Figure 1. **(A)** Displacement vectors of a pharynx GTV between two frames of the 2D sagittal cine-MR data. **(B)** P95 displacement values for the surface pixels of delineated GTVs, red and green markers show the average AP/CC displacement of the tumor during respiration. Blue markers show the difference in average tumor position over 10 minutes. **(C)** Tumor displacement in CC direction over a single dynamic MRscan.

Conclusion: Tumor displacements on both time scales were relatively small, but varied considerably between patients.

PV-0325

Retrospective self-sorted 4D-MRI for the liver

T. Van de Lindt[1], U. Van der Heide[1], J. Sonke[1]
[1]Netherlands Cancer Institute Antoni van Leeuwenhoek Hospital, Radiation Oncology, Amsterdam, The Netherlands

Purpose or Objective: There is an increasing interest in 4D-MRI for MR-guided radiotherapy. 4D-MRI methods are typically based on either an external respiratory surrogate with possible deviations from internal motion or an internal navigator channel which can disturb the image acquisition.